Adenylate cyclase A amplification and functional diversification during Polyspondylium pallidum development

Kawabe, Yoshinori; Schaap, Pauline

Published in:
EvoDevo

DOI:
10.1186/s13227-022-00203-7

Publication date:
2022

Kawabe and Schaap *EvoDevo (2022)13:18*
https://doi.org/10.1186/s13227-022-00203-7

EvoDevo

RESEARCH

Open Access

Adenylate cyclase A amplification and functional diversification during *Polyspondylium pallidum* development

Yoshinori Kawabe and Pauline Schaap*

Abstract

Background: In *Dictyostelium discoideum* (*Ddis*), adenylate cyclase A (ACA) critically generates the cAMP oscillations that coordinate aggregation and morphogenesis. Unlike group 4 species like *Ddis*, other groups do not use extracellular cAMP to aggregate. However, deletion of cAMP receptors (cARs) or extracellular phosphodiesterase (PdsA) in *Polyspondylium pallidum* (*Ppal*, group 2) blocks fruiting body formation, suggesting that cAMP oscillations ancestrally control post-aggregative morphogenesis. In group 2, the *acaA* gene underwent several duplications. We deleted the three *Ppal aca* genes to identify roles for either gene and tested whether *Ppal* shows transient cAMP-induced cAMP accumulation, which underpins oscillatory cAMP signalling.

Results: In contrast to *Ddis*, pre-aggregative *Ppal* cells did not produce a pulse of cAMP upon stimulation with the cAR agonist 2′H-cAMP, but acquired this ability after aggregation. Deletion of *Ppal aca1*, *aca2* and *aca3* yielded different phenotypes. *aca1*$^-$ cells showed relatively thin stalks, *aca2*$^-$ showed delayed secondary sorogen formation and *aca3*$^-$ formed less aggregation centers. The *aca1*$^-$*aca2*$^-$ and *aca1*$^-$*aca3*$^-$ mutants combined individual defects, while *aca2*$^-$*aca3*$^-$ and *aca1*$^-$*aca3*$^-$*aca2*$^-$ additionally showed > 24 h delay in aggregation, with only few aggregates with fragmenting streams being formed. The fragments developed into small fruiting bodies with stalk and spore cells. Aggregation was restored in *aca2*$^-$*aca3*$^-$ and *aca1*$^-$*aca3*$^-$*aca2*$^-$ by 2.5 mM 8Br-cAMP, a membrane-permeant activator of cAMP-dependent protein kinase (PKA). Like *Ddis*, *Ppal* sorogens also express the adenylate cyclases ACR and ACG. We found that prior to aggregation, *Ddis aca*$^-$*/ACG* cells produced a pulse of cAMP upon stimulation with 2′H-cAMP, indicating that cAMP oscillations may not be dependent on ACA alone.

Conclusions: The three *Ppal* replicates of *acaA* perform different roles in stalk morphogenesis, secondary branch formation and aggregation, but act together to enable development by activating PKA. While even an *aca1*$^-$*aca3*$^-$*aca2*$^-$ mutant still forms (some) fruiting bodies, suggesting little need for ACA-induced cAMP oscillations in this process, we found that ACG also mediated transient cAMP-induced cAMP accumulation. It, therefore, remains likely that post-aggregative *Ppal* morphogenesis is organized by cAMP oscillations, favouring a previously proposed model, where cAR-regulated cAMP hydrolysis rather than its synthesis dominates oscillatory behaviour.

Keywords: Excitable systems, CAMP oscillations, Adenylate cyclase A, Coordinated cell migration, Cell aggregation, Morphogenetic movement, Dictyostelia

Background

Developing organisms need to coordinate cell differentiation with the generation of form. While differentiation largely results from regulation of gene expression, form can be generated by coordinated cell movement, cell

*Correspondence: p.schaap@dundee.ac.uk

School of Life Sciences, University of Dundee, Dundee DD15EH, UK

division or changes in cell shape, either of which can act alone or in combination with others [1]. *D. discoideum* (*Ddis*) amoebas survive starvation by aggregating to form a migrating sorogen or slug, which turns into a fruiting body, consisting of spores and stalk cells. The chemotactic cell movements that cause aggregation as well as slug and fruiting body morphogenesis are organized by pulses of cAMP that are initially secreted by the most food-deprived cells and propagate as waves through the population by cAMP-induced cAMP synthesis [2–4]. The oscillating centre becomes the organizing tip of aggregates, slugs and fruiting bodies.

Dictyostelia can be subdivided into four major groups, with *Ddis* residing in group 4. The other group 4 species also use cAMP as chemoattractant [5] and are likely to use cAMP pulses to coordinate morphogenesis as well. However, this is not clear for species in the other three groups, which use the dipeptide glorin and other compounds as chemoattractant for aggregation [5–9]. Nevertheless, deletion of either cARs or PdsA from the group 2 species *P. pallidum (Ppal)* disorganized post-aggregative morphogenesis [10–12], while *D. minutum* in group 3 showed cAMP-induced cAMP synthesis and oscillatory cell movement only after aggregation [13, 14]. This suggested that non-group 4 species use cAMP oscillations to coordinate morphogenesis in the slug and fruiting body stage while using other chemoattractants for aggregation.

To test this hypothesis we deleted the three *acaA* homologs from *Ppal* individually and in combination. While single knock-outs in *aca1*, *aca2* or *aca3* showed subtle defects in primary stalk, side-branch formation and aggregation, respectively, triple *aca1*¯*aca3*¯*aca2*¯ cells were very delayed in aggregation, but still formed some small fruiting bodies after a long delay. We explored whether other dictyostelid adenylate cyclases could also participate in pulsatile cAMP signalling.

Results

Spatio-temporal expression patterns of *P. pallidum acaA* homologs

In *D. discoideum (Ddis), acaA* shows complex expression from different promoters. The promoter proximal to the coding sequence directs high expression at the slug tip, the central promoter directs low expression in the prespore region, while the most distal promoter directs high expression during aggregation [15]. *P. pallidum (Ppal)* has three *acaA* genes, *aca1*, *aca2* and *aca3* (Additional file 1: Fig. S1). Comparative transcriptomics shows that these and other *acaA* genes across taxon groups are upregulated after starvation, with group 4 *acaA* genes showing peak expression during aggregation. *Aca* genes are most highly expressed in stalk cells in groups 1–3, but in group 4 expression is highest in cup cells, which are unique to group 4 (Additional File 1: Fig. S1).

To investigate the spatial expression pattern of *Ppal aca1*, *aca2* and *aca3,* their promoter regions were fused to the *LacZ* reporter gene and transformed into *Ppal* cells. Developing structures were fixed and incubated with X-gal to visualize β-galactosidase activity. *Aca1* was not expressed during aggregation and started to be expressed weakly at the utmost tip region of the primary sorogen, and later sometimes in the tip of secondary sorogens (Fig. 1A). *Aca*2 and *aca*3 were already expressed in streaming aggregates and more strongly during post-aggregative development (Fig. 1B, C). In primary sorogens, *aca*2 was expressed throughout the structure but most strongly at the tip region. *Aca*3 expression was more specific to the tips of primary and secondary sorogens. Overall, the post-aggregative expression pattern of the three *Ppal aca*s resembles that of *Ddis acaA* with strongest expression at the sorogen tips [15, 16].

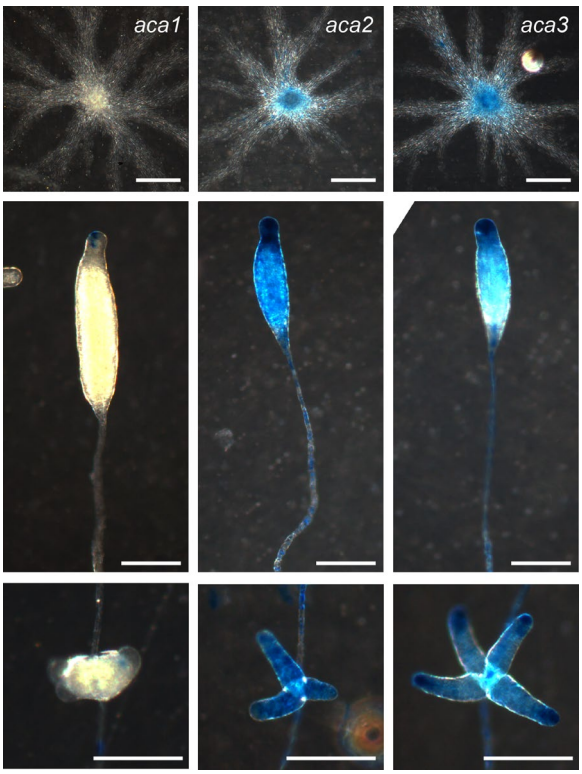

Fig. 1 Expression patterns of *P. pallidum aca* genes. *Ppal* wild-type cells were transformed with gene fusions of the *LacZ* reporter and the intergenic regions upstream of the start-codon of the *Ppal aca1*, *aca2* and *aca3* genes. The cells were developed on NN agar until streaming aggregates (top), primary sorogens (centre) and secondary sorogens (bottom) had formed and intact structures were then fixed with glutaraldehyde and stained with X-gal. Bars: 0.1 mm

Deletion of *aca genes* in *P. pallidum*

To assess the biological roles of the three *Ppal aca* genes, we replaced essential regions in each gene with the LoxP-NeoR cassette, in which *NeoR*, the single selectable marker of *Ppal* is flanked by *loxP* sites (Additional file 1: Fig. S2). The *aca1*$^-$ clones aggregated normally and formed fruiting bodies with somewhat thinner and longer stalks than those of wild type *Ppal* (Fig. 2A, D). The *aca2*$^-$ mutant aggregated and formed the primary sorogen normally but showed delayed formation of the first whorls of secondary sorogens (Fig. 2C). Such whorls arise at regular intervals when a posterior segment of the primary sorogen pinches off, while forming several regularly spaced tips, which each give rise to a small side branch. As a result, the branch-less lower stalk of *aca2*$^-$ fruiting bodies was longer than in wild-type (Fig. 2D). The *aca3*$^-$ mutant formed few aggregation centres with long streams (Fig. 2A), that partitioned into many tip-forming small aggregates that each gave rise to a small fruiting body. The central, large *aca3*$^-$ aggregate produced a normal fruiting body (Fig. 2B, D). Overall, the phenotypes of single *aca* knock-out mutants were subtle. We tried to generate double and triple *aca* knock-outs by recycling the LoxP-NeoR cassette using the cre-recombinase expression vector pA15NLS.Cre [17]. This succeeded for the *aca1*$^-$ mutant, allowing us to generate *aca1*$^-$*aca2*$^-$ and *aca1*$^-$*aca3*$^-$ double knock-outs, but not for the *aca2*$^-$ or *aca3*$^-$ knock-outs. The *aca1*$^-$*aca3*$^-$ phenotype combined features of *aca1*$^-$ and *aca3*$^-$ knock-out mutants. Similar to *aca3*$^-$, *aca1*$^-$*aca3*$^-$ formed few but

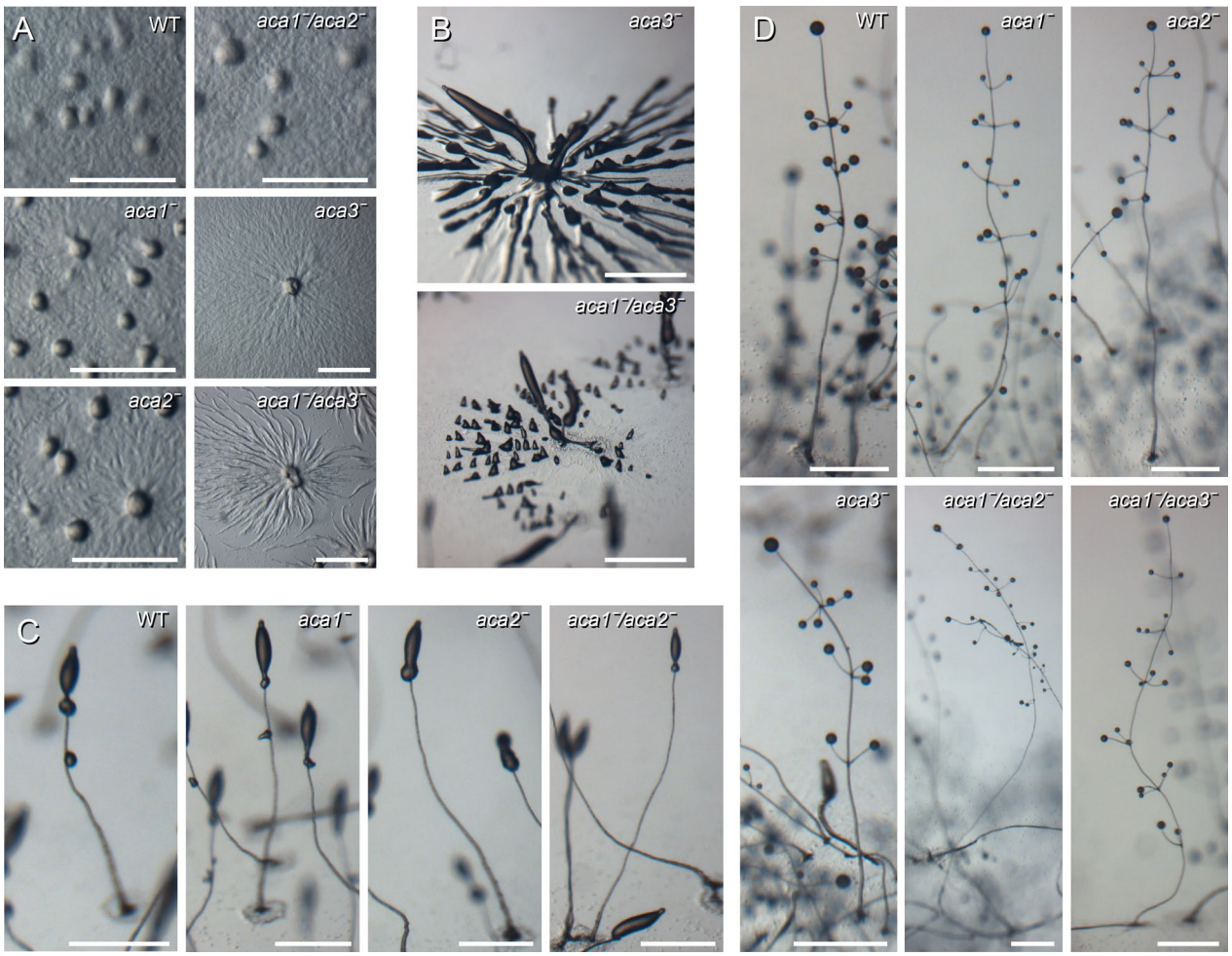

Fig. 2 Development of single *aca*, *aca1*$^-$*aca2*$^-$ and *aca1*$^-$*aca3*$^-$ mutants. Wild type (WT) *Ppal* and *aca1*$^-$, *aca2*$^-$, *aca3*$^-$, *aca1*$^-$*aca2*$^-$ and *aca1*$^-$*aca3*$^-$ knock-outs were incubated at 22 °C on NN agar at 10^6 cells/cm^2. **A** *Aggregation:* the images show aggregates after 6 h or 8 h (*aca3*$^-$ and *aca1*$^-$*aca3*$^-$) of starvation. Bars: 1 mm. **B** *Tip formation:* aggregation streams of *aca3*$^-$ and *aca1*$^-$*aca3*$^-$ forming tips at 20 h. Bars: 1.0 mm. **C** *Whorl mass separation*: *aca1*$^-$, *aca2*$^-$ and WT at 20 h and *aca1*$^-$*aca2*$^-$ at 28 h of starvation. Bars: 0.5 mm. **D** *Fruiting bodies:* WT, *aca1*$^-$, and *aca2*$^-$ had formed mature fruiting bodies at 28 h of starvation, while *aca3*$^-$ and *aca1*$^-$*aca3*$^-$ took 32 h and *aca1*$^-$*aca2*$^-$ 48 h to complete their fruiting bodies. Bars: 0.5 mm

large streaming aggregates (Fig. 2A, B), while the fruiting bodies showed thinner and longer stalks, like the *aca1*¯ mutants (Fig. 2D). The *aca1*¯*aca2*¯ cells aggregated and formed primary sorogens normally. However, the separation of the first whorl only occurred after 28 h of starvation, when WT, *aca1*¯, and *aca2*¯ had already formed fruiting bodies (Fig. 2C). As a result, *aca1*¯*aca2*¯ made very tall fruiting bodies with side branches only at the upper stalk (Fig. 2D).

The failure to recycle LoxP-NeoR cassette *of aca2*¯ or *aca3*¯ mutants was probably due to limited selectability of cells transformed with pA15NLS.Cre with its G418 selection cassette. We found that *Ppal* growth is also inhibited by the antibiotic Nourseothricin. This allowed us to use a Cre-recombinase expression vector pDM1483 [18] with a Nourseotricin selection cassette to eliminate LoxP-NeoR from *aca3*¯ and *aca1*¯*aca3*¯ and to generate *aca3*¯*aca2*¯ and *aca1*¯*aca3*¯*aca2*¯ knock-outs.

Compared to wild-type, *aca1*¯*aca2*¯, *aca1*¯*aca3*¯ and single *aca* knock-outs, which all initiated aggregation within 8 h of starvation, the *aca3*¯*aca2*¯ mutant only started to aggregate at 24 h or later (Fig. 3A). Only few aggregation foci were formed, which attracted very long aggregation streams. Starting from the initial (small) focus, mounds appeared at intervals within the streams, which each attracted downstream cells. Each of these mounds gave rise to a small, branched fruiting body, which, similar to *aca2*¯, showed a longer whorl-free lower stalk (Fig. 3B). The *aca1*¯*aca3*¯*aca2*¯ phenotype combined features of the *aca1*¯*aca2*¯ and the *aca3*¯*aca2*¯ mutant. Similar to *aca3*¯*aca2*¯, aggregation was much delayed with long streams appearing only after 24–48 h of starvation (Fig. 3A), which eventually broke up and gave rise to small fruiting bodies. These fruiting bodies showed delayed side-branch formation, like *aca1*¯*aca2*¯ (Fig. 3B). Staining of the *aca1*¯*aca3*¯*aca2*¯ stalk and spore cells with the cellulose dye Calcofluor showed that it formed a normal primary and secondary stalk and elliptical spores encapsulated in cellulose walls (Fig. 3C), and this was also the case for all other *aca*¯ mutants (not shown).

To investigate whether the aggregation phenotypes of the *aca3*¯*aca2*¯ or *aca1*¯*aca3*¯*aca2*¯ mutants were cell-autonomous, the mutants were developed as chimeras with wild-type cells. Introduction of 10% wild-type cells was sufficient to restore delayed aggregation of both mutants (Fig. 3A). The mixtures aggregated within 8 h of starvation-like wild-type cells, but still formed larger aggregation streams. In addition, the formation of secondary sorogens in *aca1*¯*aca3*¯*aca2*¯ chimeras with wild-type was not as delayed as in *aca1*¯*aca3*¯*aca2*¯ alone, resulting in formation of more normal fruiting bodies (Fig. 3B). These experiments show that the defects in aggregation and whorl separation of the *aca*¯ mutants are non-cell autonomous.

We also tested microcyst formation in *aca* knock-out mutants. Incubation with 0.2 M sorbitol for 24 h induced cyst formation in both wild type and *aca1*¯*aca3*¯*aca2*¯ to the same degree (Additional File 1: Fig. S3), indicating that the *aca* genes are not required for encystation.

Restoration of *aca1*¯*aca3*¯*aca2*¯ aggregation by 8Br-cAMP.

The strongly reduced initiation of aggregation centres and extensive delay in aggregation of both the *aca3*¯*aca2*¯ and *aca1*¯*aca3*¯*aca2*¯ was unexpected, since *Ppal* does not use cAMP as attractant for aggregation, but most likely glorin [5, 9]. However, both *Ddis* and *Ppal* require PKA activity and, therefore, likely intracellular cAMP to develop competence for aggregation [19, 20]. To investigate whether lack of PKA activation due to the absence of intracellular cAMP cause the aggregation abnormalities in *aca3*¯*aca2*¯ and *aca1*¯*aca3*¯*aca2*¯, *aca1*¯*aca3*¯*aca2*¯ cells were developed on agar containing 2.5 mM 8Br-cAMP, a membrane-permeant PKA agonist. While without 8Br-cAMP cells had not yet started to aggregate after 24 h of starvation, the 8Br-cAMP treated cells initiated many aggregation centres and almost completed aggregation within 6 h (Fig. 4). The aggregates remained, however, blocked in the mound stage and did not form fruiting bodies. This was, however, also the case for most *Ppal* WT aggregates developed on 8Br-cAMP agar. These results show that the *aca1*¯*aca3*¯*aca2*¯ aggregation defect was likely caused by insufficient intracellular cAMP for PKA activation.

cAMP relay in *Ppal* and in *Ddis aca-/ACG* cells

Despite the loss of all ACA activity, the *aca1*¯*aca3*¯*aca2*¯ cells still made relatively normal fruiting bodies after a long delay. cAMP-induced excitation and adaptation of ACA underpins pulsatile cAMP signalling and wave propagation in *Ddis* [21, 22], with cAMP receptors (cARs) and extracellular cAMP phosphodiesterase (PdsA) as essential components to, respectively, detect secreted cAMP and to hydrolyse it between pulses [23–25]. From earlier findings that *cAR* or *pdsA* null mutants in *Ppal* were specifically defective in fruiting body morphogenesis [11, 12], we concluded that cAMP waves mediated this process as they do in *Ddis* [4]. The present data imply that this is either not the case, or that the *aca1*¯*aca3*¯*aca2*¯ cells have a means to compensate for loss of ACA activity.

To investigate whether *Ppal* also shows transient cAMP-induced cAR mediated accumulation of cAMP, we stimulated wild-type *Ppal* cells at different stages of development with the cAR agonist 2'H-cAMP in the presence of the PdsA inhibitor DTT

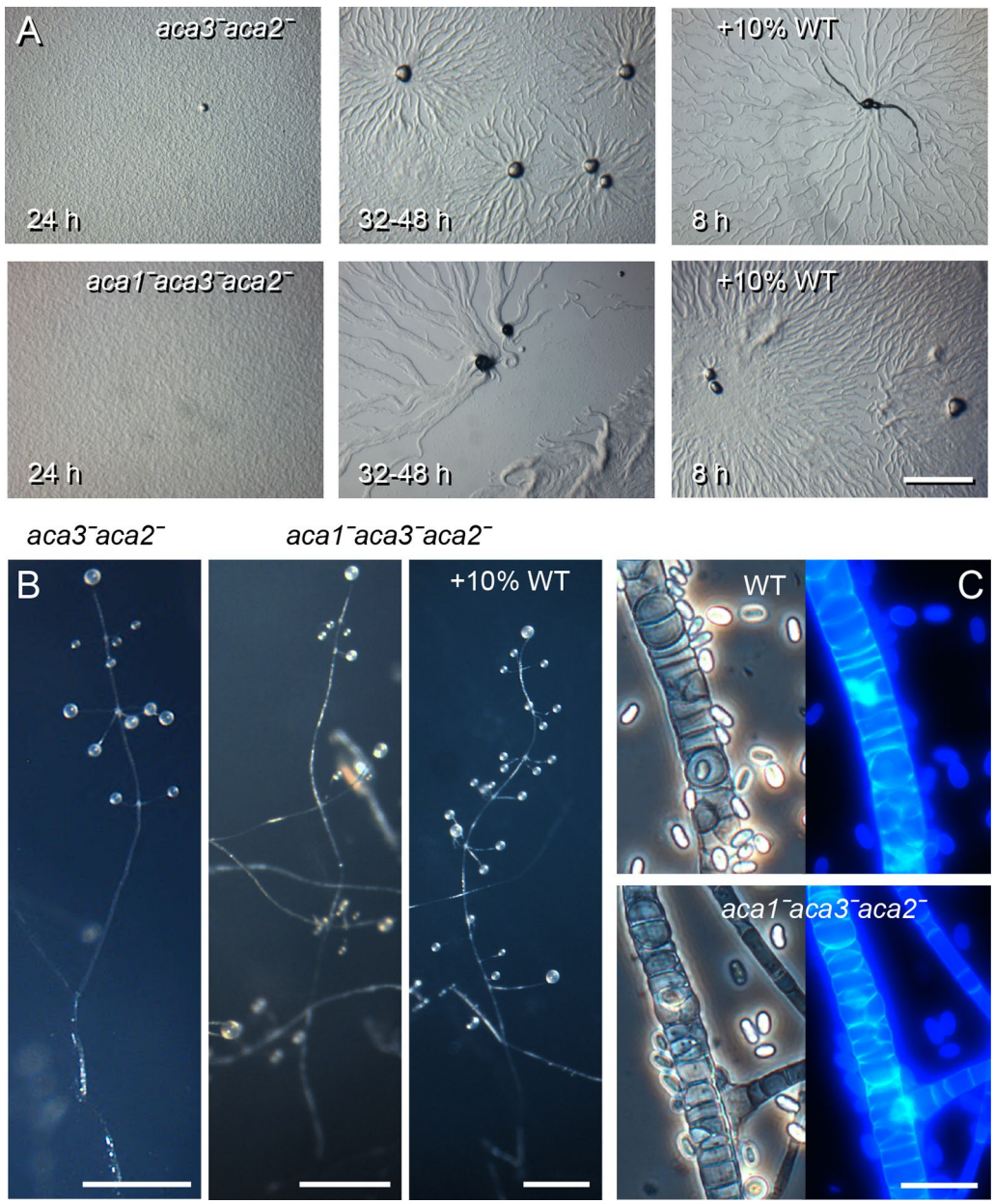

Fig. 3 Development of *aca3¯aca2¯* and *aca1¯aca3¯aca2¯ mutants.* **A** *Aggregation: Ppal aca3¯aca2¯* and *aca1¯aca3¯aca2¯* were starved on NN agar at 10^6 cells/cm^2 on their own or mixed with 10% wild-type *Ppal* for the indicated time periods. Bar: 1 mm. **B** *Fruiting bodies:* the cells were developed into fruiting bodies, which were imaged in situ. Bars: 0.5 mm. **C** *Spore and stalk cells: Ppal* WT and *aca1¯aca3¯aca2¯* fruiting bodies were transferred to 0.001% Calcofluor and imaged under phase contrast (left) and epifluorescence (right). Bar: 20 µm

[26]. Figure 5A shows that cells at all stages contain a basal level of 3–6 pmol cAMP/mg protein. Starving cells or cells from streaming aggregates showed none or marginal responses to 2'H-cAMP, while cells from tipped mounds showed a 5 pmol/mg protein increase in cAMP, which then levelled off. However, cells from dissociated sorogens showed transient increase that peaked after 3 min after stimulation at 11 pmol above basal levels and then decreased to 5 pmol. These data indicate that *Ppal* can relay a pulse of cAMP, but only after tips and sorogens have formed. In *Ddis*, which unlike *Ppal* also uses cAMP to aggregate, cAMP relay is highest at the aggregation stage [27]. We could not meaningfully measure 2'H-cAMP-induced cAMP accumulation in the *aca1¯aca3¯aca2¯* cells, because only few aggregates are formed at different times,

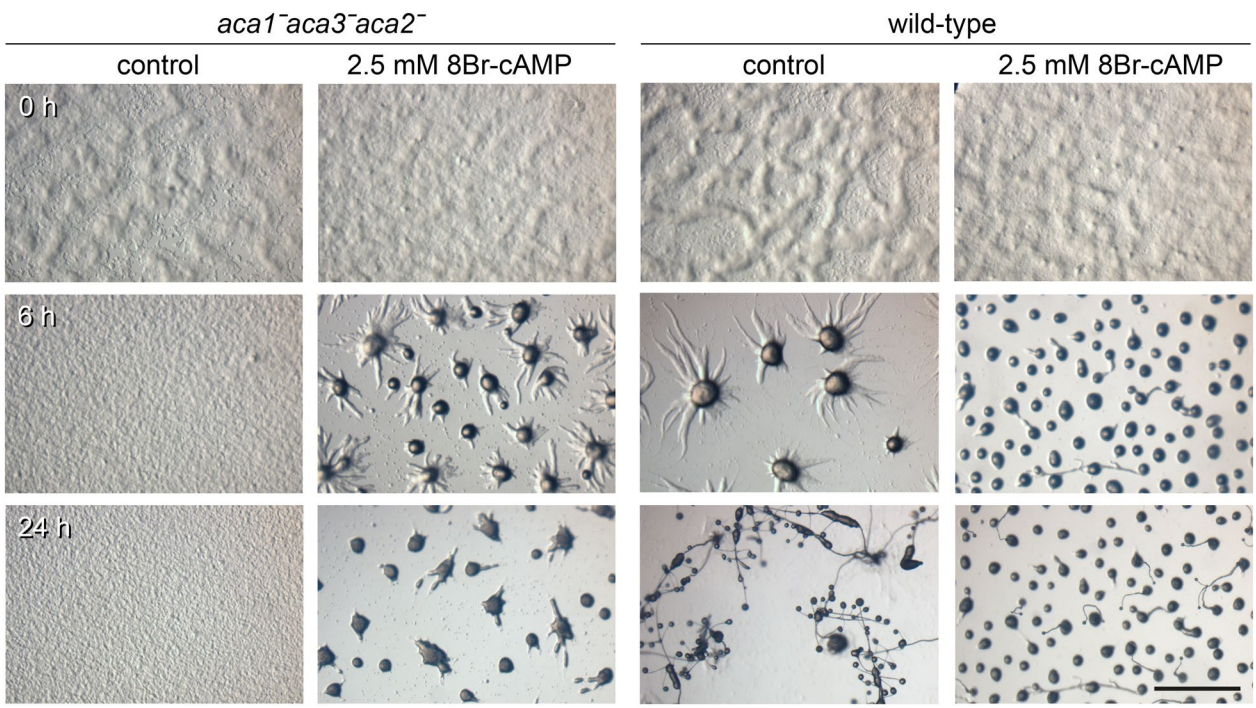

Fig. 4 Effect of 8Br-cAMP on aggregation of *aca1¯aca3¯aca2¯* cells *Ppal aca1¯aca3¯aca2¯* and wild-type cells were incubated for 24 h on NN agar with and without 2.5 mM 8Br-cAMP and imaged in situ at the indicated timepoints. Bar: 1 mm

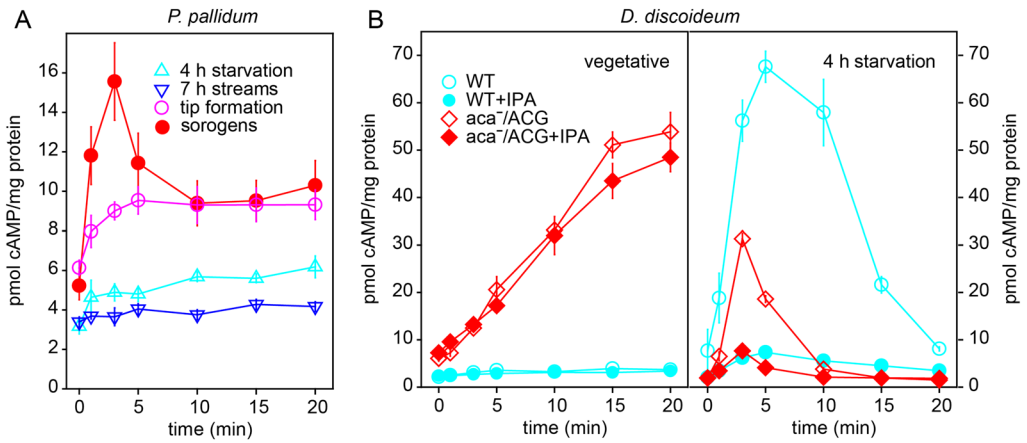

Fig. 5 cAMP relay in *Ppal* wild-type and *Ddis aca¯/ACG*. ***A*** *P. pallidum. Ppal WT* was starved on agar for 4 h or until streaming aggregates, tipped mounds and aerially lifted sorogens had formed. Structures were gently dissociated, resuspended in PB to 10^8 cells/ml and stimulated at t = 0 min with 10 µM 2'H-cAMP and 5 mM DTT. Reactions were terminated with 1.75% perchloric acid at the indicated timepoints and cAMP was assayed by isotope dilution assay. ***B*** *D. discoideum* Vegetative WT AX3 and *aca¯/ACG* cells, and cells starved on NN agar for 4 h were resuspended in PB to 10^8 cells/ml and stimulated with 5 µM 2'H-cAMP and 5 mM DTT in the presence and absence of 1 mM IPA. Reactions were terminated as above, and cAMP was assayed. Data were standardized to the protein content of the cell suspensions and represent means and SE of six experiments performed in triplicate for *Ppal* sorogens and two experiments in triplicate for other stages and cell lines. The experiments in panel B were performed twice more in triplicate with *aca¯/ACG* cells in the absence of IPA, with similar results

which then fragment and fairly rapidly mature into fruiting bodies. This means that at any time only a very small fraction of cells is in the sorogen stage.

Apart from Aca1, Aca2 and Aca3, two other adenylate cyclases, AcgA and AcrA are expressed in *Ppal* sorogens [28]. The experiment in Fig. 5A does not identify the adenylate cyclase responsible for the cAMP increase. While currently not feasible in *Ppal*, a *Ddis acaA* knock-out is available that expresses *AcgA* (ACG) from the constitutive actin 15 promoter [29]. During growth, this mutant synthesizes cAMP at a constant rate [30], but it is unknown whether cAMP synthesis comes under cAR regulation at a later stage. We compared 2'H-cAMP-induced cAMP accumulation between *Ddis* wild-type and *aca*¯*/ACG* cells in vegetative and 4 h starved cells, which are just starting to aggregate. To validate that the observed responses are mediated by *Ddis* cAR1, we included the cAR1 antagonist 2′3′-O-isopropylidene adenosine (IPA) in control assays. Figure 5B shows that wild-type *Ddis* shows no 2'H-cAMP-induced cAMP accumulation in the vegetative stage and a 70 pmol/mg protein increase in 4 h starved cells that peaks at 5 min. This response is almost completely inhibited by IPA. Vegetative aca¯/ACG cells show a steady increase in cAMP levels after addition of 2'H-cAMP/DTT that is only slightly reduced in the presence of IPA. However, 4 h starved aca¯/ACG cells show a faster transient increase of cAMP that peaks at 3 min after 2′H-cAMP/DTT stimulation. This response is also strongly reduced by IPA. These data indicate that in early aggregating *Ddis* cells, ACG is also controlled by cAR stimulation. The apparent ability of other adenylate cyclases than ACA to participate in transient cAR mediated cAMP accumulation provides some resolution for the contrasting effects on *Ppal* fruiting body morphogenesis of *aca* deletion on one hand, and *cAR* or *pdsA* deletion on the other.

Discussion

Gene amplification of *aca* genes and their expression in *P. pallidum*

Representative species of the *Dictyostelium* taxon groups 1, 3 and 4 have a single gene each of the adenylate cyclases *acaA*, *acrA* and *acgA*, but in taxon group 2, the ancestral *acaA* gene was amplified twice in *Ppal* and three times in *A. subglobosum* (Additional File 1, Fig. S1). In *Ddis*, a signaling network that critically incorporates ACA, cAR1 and PdsA generates the cAMP pulses that coordinate aggregation and cell movement in the multicellular stage [24, 29]. Deletion of the two *Ppal car* genes, *carA* and *carB,* or its single *pdsA* gene had no effect on aggregation but disorganized the subsequent formation of sorogens and fruiting bodies [11, 12]. This suggested that similar to *Ddis*, *Ppal* multicellular morphogenesis is organized by cAMP pulses. The *Ppal* attractant for aggregation is likely the dipeptide glorin, since starving *Ppal* cells chemotactically respond to glorin [9] and their aggregation is disrupted by including glorin in the supporting agar [5].

We here show that *Ppal aca1* was poorly expressed and only visible in the tips of primary and secondary sorogens, while *aca2* and *aca3* expression was already visible in aggregates. Both genes were preferentially expressed in tip and stalk cells, but *aca2* was also expressed in prespore cells. The latter expression likely explains why double loss of *acrA* and *acgA*, which in *Ddis* leads to complete loss of prespore and spore differentiation [31], only mildly affects *Ppal* sporulation [20]. The post-aggregative expression pattern of either *Ppal aca* resembles that of *Ddis acaA*, which is also preferentially expressed in the organizing tip, from which the organizing cAMP waves emanate [4, 15, 16].

Ppal aca3 is required for PKA activation and early development

Deletion of individual *Ppal aca* genes caused subtle developmental defects (summarized in Table 1), with

Table 1 Phenotypes of *Ppal aca* knock-outs

Mutant	Phenotype	
	Aggregation	Morphogenesis
aca1¯	Normal	Somewhat thinner and longer stalks
aca2¯	Normal	Delayed whorl separation
aca3¯	Delayed, few centers, long streams	Normal
aca1¯*aca2*¯	Normal	Long whorl-free lower stalk, thin tall fruiting bodies
aca1¯*aca3*¯	Delayed, few centers, long streams	Somewhat thinner and longer stalks
aca3¯*aca2*¯	Very delayed, few centres, long streams	Long whorl-free lower stalk
aca1¯*aca3*¯*aca2*¯	Very delayed, very few centres, long streams	Thin tall fruiting bodies, whorls only near top

aca1¯ displaying longer, thinner stalks, *aca2*¯ delayed separation of the first whorl from the main sorogen and *aca3*¯ showing delayed and reduced formation of aggregation centres, giving rise to extensive streaming (Fig. 2). Double *aca1*¯*aca2*¯ and *aca1*¯*aca3*¯ knock-outs combined the phenotypes of the individual knock-outs, but *aca3*¯*aca2*¯ was very delayed in aggregation and like *aca1*¯*aca3*¯*aca2*¯ only formed a few aggregates on an entire plate of cells. The latter mutant did, however, form small fruiting bodies with some whorls of side branches near the top after a very long delay (Fig. 3). Both the delayed aggregation and delayed secondary sorogen formation are non-cell autonomous defects as they are restored by chimeric development of the mutants with 10% wild-type cells.

The delay in aggregation caused by loss of *aca3* was somewhat enigmatic, since no such delay occurred in *Ppal carA*¯*carB*¯ or *pdsA*¯ mutants, which cannot detect or hydrolyse extracellular cAMP, respectively. Exposure of the *aca1*¯*aca3*¯*aca2*¯ mutant to the membrane-permeant PKA agonist 8Br-cAMP restored normal aggregation (Fig. 4) indicating that Aca3 provides cAMP for activation of PKA in early development. Because defective aggregation of *aca3*¯ is also restored by wild-type cells, this likely means that PKA induces genes required for glorin synthesis. In early *Ddis* development PKA also acts to induce expression of aggregation genes [19].

The *Ppal aca* genes are not essential for post-aggregative morphogenesis

Despite its long delay in forming aggregates *Ppal aca1*¯*aca3*¯*aca2*¯ cells were still able to form relatively normal fruiting bodies with stalk and spore cells. In view of observations that *Ppal carA*¯*carB*¯ or *pdsA*¯ cells are highly defective in fruiting body morphogenesis, this suggests that perhaps a static gradient of cAMP produced by ACR or ACG is sufficient to organize morphogenesis or that either or both of these adenylate cyclases can also participate in an oscillatory network. When expressed from the constitutive A15 promoter in an *aca*¯ background, *Ddis* ACG displays a fairly high level of constitutive activity in the growth stage that is activated by high osmolarity [32]. In wild-type *Ddis*, ACG has an overlapping role with ACR in induction of spore formation and inhibition of spore germination [31, 33]. In *Ppal* ACG and ACR critically regulate encystation, but their role in sporulation is less pronounced [20], which may be due to the additional activity of Aca1, 2 and 3 in sorogens.

ACG mediates cAMP stimulated transient cAMP accumulation

Ppal cells at the sorogen stage show transient 2′HcAMP-induced cAMP synthesis (Fig. 5A), consolidating evidence from *Ppal car*¯ and *pdsA*¯ mutants that cAMP pulses coordinate postaggregative morphogenesis [11, 12], but the *Ppal aca1*¯*aca3*¯*aca2*¯ mutant still makes fruiting bodies, suggesting that this is not the case. To resolve this conundrum, we explored whether other adenylate cyclases might mediate pulsatile signaling. We found that when aggregation competent *Ddis aca*¯*/ACG* cells are stimulated with 2′HcAMP, ACG mediates a transient accumulation of cAMP (Fig. 5B). Like ACA mediated transient cAMP synthesis, the response is inhibited by the cAR antagonist IPA, indicating that it is mediated by cARs. The experiment shows that at least one of the other dictyostelid adenylate cyclases could also give rise to oscillatory cAMP signalling, which provides some resolution to the conundrum.

How the apparent transient ACG activation occurs is unresolved. Oscillatory cAMP signalling depends on both positive and negative feedback loops acting on cAMP production (Fig. 6). ACA activation involves positive feedback loop, where cAMP synthesized by ACA process binds to cAR1 and initiates a multistep process that causes activation of ACA (see [34]. Negative feedback on ACA may involve PIP3, one of the activating intermediates, also causing inhibition of ACA after a delay [35]. In an alternative model (Fig. 6B), the positive feedback loop involves both cAMP activation of ACA, as above, and of the protein kinase ERK2, which next inactivates the intracellular cAMP phosphodiesterase RegA, enabling cAMP to increase. The negative loop involves PKA activation by cAMP synthesized by ACA, inactivation of ERK2 and thereby activation of RegA [36]. In this model it is mostly cAMP degradation that is under

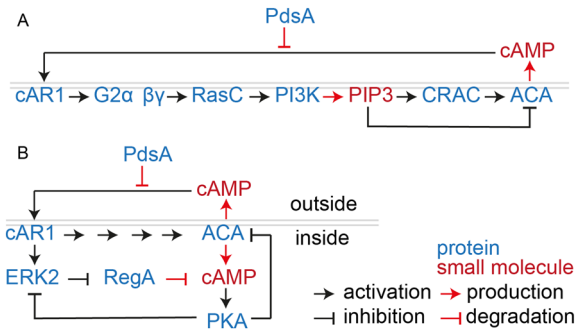

Fig. 6 Proposed models for ACA mediated oscillatory cAMP signalling See main text for explanation. Abbreviations: *PdsA* phosphodiesterase A, *cAR1* cAMP receptor 1, *G2*: heterotrimeric G-protein 2, *RasC* small GTPase C, *PI3K*: phosphoinositide 3-kinase, *PIP3* phosphatidylinositol-(3,4,5)-trisphosphate, *CRAC* cytosolic regulator of adenylate cyclase, *ACA* adenylate cyclase A, *ERK2* extracellular signal-regulated kinase 2, *RegA* cAMP phosphodiesterase with response regulator, *PKA* cAMP dependent protein kinase. Schematics are based on Fig. 6 in [35] and Fig. 2 in [36]

positive and negative feedback regulation, making it conceivable that a constitutively active adenylate cyclase-like ACG or ACR could still display apparent transient activation.

Conclusions

In *Ddis,* cAMP waves produced by ACA and emanating from aggregation centres and organizing tips control both aggregation and post-aggregative morphogenesis. We here investigated ACA function in *Ppal*, which likely uses glorin for aggregation. *Ppal* has 3 *aca* genes, which similar to *Ddis aca* are most highly expressed in the organizing tip. Deletion of either gene causes different but relatively subtle changes in aggregation and post-aggregative morphogenesis, while deletion of all three *aca* genes causes a long delay in aggregation with only few centres being formed that attracted long streams of amoebas. The fragmenting streams eventually gave rise to small fruiting bodies. Timely aggregation was restored by including the PKA agonist 8Br-cAMP in the substratum, indicating that in early development the *Ppal* ACAs are needed to activate PKA.

While the formation of fruiting bodies by the *Ppal aca1*$^{-}$*aca3*$^{-}$*aca2*$^{-}$ mutant argues against a role for ACAs and thereby oscillatory cAMP signalling in fruiting body morphogenesis, several lines of evidence indicate the opposite. 1. Loss of other components that are essential for cAMP oscillations, such as cARs or pdsA disorganizes morphogenesis. 2. Post-aggregative *Ppal* cells produce a cAMP pulse when stimulated with 2′H-cAMP, a cAMP receptor agonist. 3. In *Ddis* other adenylate cyclases, such as ACG also mediate transient 2′H-cAMP-induced cAMP accumulation, at a stage when cARs and PdsA are also present.

Overlapping roles of ACG and ACR were detected in *Ddis* sporulation [31] and *Ppal* encystation, while the *Ppal* ACAs were proposed to overlap with ACG and ACR in induction of sporulation [20]. The current study provides hints that ACG and possibly ACR in turn overlap with ACA in morphogenetic signalling. Altogether, ACA, ACG and ACR may ancestrally have been less specialized and acquired their specific roles in the course of dictyostelid evolution by expression in different cell types and interaction with proteins specific to that cell type.

Methods

Growth and development.

P. pallidum PN500 (*Ppal*) was routinely grown in association with *Escherichia coli* on LP agar or 1/5th SM agar (Formedium, UK). For multicellular development, cells were harvested in 20 mM K-phosphate, pH 6.5 (KK2), washed free from bacteria and incubated at 10^6 cells/cm^2 and 22 °C on NN agar (1.5% agar in 8.8 mM KH_2PO_4 and 2.7 mM Na_2HPO_4) until the desired developmental stages had been reached. *D. discoideum* (*Ddis)* AX3 and *aca*$^{-}$*/ACG* cells [29] were grown in HL5 axenic medium, which was supplemented with 20 µg/ml G418 for *aca*$^{-}$*/ACG.*

DNA constructs and transformation

Ppal Aca promoter-lacZ constructs and analysis

To construct a gene fusion of the *Ppal aca1* promoter and *lacZ*, an *aca1* (PPL_01657) fragment 3511 nt upstream and 93 nt downstream of the start ATG was amplified from *Ppal* gDNA using primers Pp-ACA1-P52X with *Xba*I site and Pp-ACA1-P32. The fragment was digested with *Xba*I and *Bam*HI (using an internal *Bam*HI site) and ligated into the *Bgl*II/*Xba*I digested pDdGal17 [37], yielding pPpACA1-LacZ. The *aca2* (PPL_12370) 3.8 kb 5'intergenic region (− 3743 to + 86) was amplified using primers Pp-ACA2-P51E and Pp-ACA2-P31B that harbour *Eco*RI and *Bam*HI, respectively. The *Eco*RI/*Bam*HI digested PCR product was ligated into the *Eco*RI/*Bgl*II digested pDdGal16 [37], yielding vector pPpACA2-LacZ. The *aca3* (PPL_10658) 2.6 kb 5′ intergenic region (− 2502 to + 50) was amplified using primers Pp-ACA3-P52X and Pp-ACA3-P32B that harbour *Xba*I and *Bam*HI, respectively. The *Xba*I/*Bam*HI digested PCR product was ligated into similarly digested pDdGal17, yielding vector pPpACA3-LacZ. After validation of the plasmids by DNA sequencing, they were transformed into *Ppal* wild-type cells. Transformants were selected at 300 µg/ml G418 [38] and pools of 7–10 transformed clones were developed into multicellular structures on dialysis membrane, supported by NN agar. β-galactosidase activity was visualized with X-gal in the structures, as described previously [11, 39].

Ppal gene knock-out constructs

To disrupt *Ppal aca1* (PPL_01657), an *aca1* fragment was amplified from *Ppal* PN500 genomic DNA using primers Pp-ACA-51H and Pp-ACA-31B (Additional file 1: Table S1) that harbour *Hind*III and *Bam*HI restriction sites, respectively. The fragment was cloned into *Bam*HI/*Hind*III digested pBluescript SK + which was next digested with EcoRV. The LoxP-NeoR cassette of pLoxNeoIII [12] was excised with BamHI and HindIII, filled in with Klenow polymerase, and ligated into the EcoRV digested *aca1* plasmid, yielding vectors pACA1-KO1 and pACA1-KO2, with loxP-NeoR inserted in *aca1* in forward and reverse orientation, respectively, and flanked by 2307 bp 5′UTR and 5'*aca1* sequence and 1414 bp 3'*aca1* sequence (Additional file 1: Fig. S2A). pACA1-KO2 was used for gene disruption.

To disrupt *Ppal aca2* (PPL_12370), an *aca2* fragment was amplified using primers Pp-ACA2-51 K and

Pp-ACA2-31S (Additional file 1: Table S1) that harbour *Kpn*I and *Sac*I sites, respectively. The fragment was cloned into *Kpn*I/*Sac*I digested pBluescript SK+ which was next digested with *Bam*HI/*Sal*I. LoxP-NeoR was excised with *Bam*HI/*Sal*I from pLoxNeoIII and ligated into the *Bam*HI/*Sal*I digested *aca2* plasmid, yielding vector pACA2-KO with LoxP-NeoR flanked by 1918 bp 5'*aca2* sequence and 3086 bp 3'*aca2* and 3'UTR sequence (Additional file 1: Fig. S2B).

To disrupt *Ppal aca3* (PPL_10658), two *aca3* sequences, A and B, were amplified using primer pair Pp-ACA3-51 K/Pp-ACA3-31X, that harbour *Kpn*I and *Xba*I sites for A and primer pair Pp-ACA3-52B/Pp-ACA3-32X with *Bam*HI and *Xba*I sites for B, respectively. Fragment A was digested with *Kpn*I/*Sal*I (using an internal *Sal*I site) and inserted into *Kpn*I/*Sal*I digested pLox-NeoIII, and next *Bam*HI/*Xba*I digested fragment B was inserted into the *Bam*HI/*Xba*I sites of the resulting vector, yielding pACA3-KO with 2042 bp 5' *aca3* sequence and 2531 bp 3' *aca3* and 3'UTR sequence. (Additional file 1: Fig. S2C).

Ppal cells were transformed by electroporation with the linearized vectors according to established procedures [38]. Genomic DNA was isolated from G418 resistant clones and analyzed by PCR and Southern blots to diagnose gene disruption by homologous recombination (Additional file 1: Fig. S2).

To generate double *aca1*¯*aca2*¯ or *aca1*¯*aca3*¯ knockouts, the loxP-NeoR cassette was removed from *aca1*¯ by transient transformation with pA15NLS.Cre [17]. Cells that had regained sensitivity to G418 were then transformed with the pACA2-KO or pACA3-KO plasmids. This strategy did not work for the *aca2*¯ and *aca3*¯ knockouts. To generate an *aca3*¯*aca2*¯ double and *aca1*¯*aca3*¯*aca2*¯ triple knockout, *aca3*¯ and *aca1*¯*aca3*¯ were transformed with pDM1483 [18], which harbours cassettes for Nourseothricin selection and cre-recombinase expression. Transformants were selected after growth for 3–5 days in the presence of 300 µg/ml Nourseothricin, and, after replica-plating, selected for G418 sensitivity and transformed with the pACA2-KO vector. All gene knock-outs were diagnosed by PCR and/or Southern blot (Additional file 1: S2).

cAMP relay assays

To measure cAMP-induced cAMP accumulation, *Ppal* cells were resuspended in PB (10 mM Na/K-phosphate, pH 6.5) at 10^8 cells/ml, dispensed as 25 µl aliquots in microplate wells and, stimulated with 5 µl of 60 µM 2'H-cAMP (2'-deoxyadenosine 3':5'-cyclic monophosphate, Sigma-Aldrich, in 30 mM DTT (dithiothreitol, Sigma-Aldrich) and shaken at 100 rpm and 21 °C. Reactions were terminated by addition of 30 µl of 3.5% (v/v) perchloric acid. *Ddis* cells additionally received 3 µl of 10 mm IPA (2',3'-O-isopropylideneadenosine, Sigma-Aldrich) in 10% (v/v) (DMSO) dimethylsulfoxide, Sigma-Aldrich) or 3 µl 10% DMSO (controls) and were stimulated with 3 µl 50 µM 2'H-cAMP in 50 mM DTT. For cAMP assay, samples were neutralized by addition of 15 µl of 50% saturated $KHCO_3$ and 75 µl of cAMP assay buffer (4 mM EDTA in 150 mM K phosphate, pH 7.5). Protein and perchlorate were precipitated by centrifugation for 5 min at 2000 ×g and cAMP was assayed in 50 µl of supernatant by isotope dilution assay using purified PKA regulatory subunit from beef heart as cAMP-binding protein and [2,8-^{3}H]cAMP (Perkin–Elmer) as competitor [26, 40].

Supplementary Information

The online version contains supplementary material available at https://doi.org/10.1186/s13227-022-00203-7.

Additional file 1: Figure S1. *acaA* genes across Dictyostelia. **Figure S2.** Schematics and diagnosis of *Ppal aca1*, *aca2* and *aca3* knock-outs. **Figure S3.** Encystation. **Table S1.** Oligonucleotide primers used in this work.

Author contributions

YK and PS designed the study, YK performed most experimental work, analyzed the data and wrote the first draft of the manuscript. PS supervised the work, performed the cAMP relay experiments and prepared the final draft. All authors read and approved the final manuscript.

Funding

This research was funded by BBSRC grant BB/K000799/1 and ERC grant 74228. The BBSRC and ERC grants were used at initial and later phases of the work to fund the salary of YK and the materials to carry out the study.

Availability of data and materials

All data generated or analyzed during this study are included in this article and Additional file 1. The DNA constructs and knock-out cell lines produced in the study will be deposited in the *Dictyostelium* Stock Centre http://dictybase.org/StockCenter/StockCenter.html

Declarations

Ethics approval and consent to participate

Not applicable.

Consent for publication

Not applicable.

Competing interests

The authors declare that they have no competing interests.

Received: 23 July 2022 Accepted: 28 September 2022
Published online: 19 October 2022

References

1. Montell DJ. Morphogenetic cell movements: diversity from modular mechanical properties. Science. 2008;322(5907):1502–5.
2. Dinauer MC, MacKay SA, Devreotes PN. Cyclic 3',5'-AMP relay in *Dictyostelium discoideum* III The relationship of cAMP synthesis and secretion during the cAMP signaling response. JCell Biol. 1980;86:537–44.

3. Wang M, Aerts RJ, Spek W, Schaap P. Cell cycle phase in *Dictyostelium discoideum* is correlated with the expression of cyclic AMP production, detection, and degradation. DevBiol. 1988;125:410–6.
4. Singer G, Araki T, Weijer CJ. Oscillatory cAMP cell-cell signalling persists during multicellular *Dictyostelium* development. Commun Biol. 2019;2:139.
5. Romeralo M, Skiba A, Gonzalez-Voyer A, Schilde C, Lawal H, Kedziora S, Cavender JC, Glockner G, Urushihara H, Schaap P. Analysis of phenotypic evolution in dictyostelia highlights developmental plasticity as a likely consequence of colonial multicellularity. Proc Biol Sci. 2013;280(1764):20130976.
6. Shimomura O, Suthers HLB, Bonner JT. Chemical identity of the acrasin of the cellular slime mold *Polysphondylium violaceum*. Proc Natl Acad Sci USA. 1982;79:7376–9.
7. De Wit RJW, Konijn TM. Identification of the acrasin of *Dictyostelium minutum* as a derivative of folic acid. Cell Differ. 1983;12:205–10.
8. Van Haastert PJM, De Wit RJW, Grijpma Y, Konijn TM. Identification of a pterin as the acrasin of the cellular slime mold *Dictyostelium lacteum*. Proc Natl Acad Sci USA. 1982;79:6270–4.
9. Asghar A, Groth M, Siol O, Gaube F, Enzensperger C, Glockner G, Winckler T. Developmental gene regulation by an ancient intercellular communication system in social amoebae. Protist. 2011;163:25–37.
10. Kawabe Y, Kuwayama H, Morio T, Urushihara H, Tanaka Y. A putative serpentine receptor gene *tasA* required for normal morphogenesis of primary stalk and branch structure in *Polysphondylium pallidum*. Gene. 2002;285(1–2):291–9.
11. Kawabe Y, Morio T, James JL, Prescott AR, Tanaka Y, Schaap P. Activated cAMP receptors switch encystation into sporulation. Proc Natl Acad Sci USA. 2009;106(17):7089–94.
12. Kawabe Y, Weening KE, Marquay-Markiewicz J, Schaap P. Evolution of self-organisation in dictyostelia by adaptation of a non-selective phosphodiesterase and a matrix component for regulated cAMP degradation. Development. 2012;139(7):1336–45.
13. Schaap P, Konijn TM, Van Haastert PJM. cAMP pulses coordinate morphogenetic movement during fruiting body formation of *Dictyostelium minutum*. Proc Natl Acad Sci USA. 1984;81:2122–6.
14. Schaap P. cAMP relay during early culmination of *Dictyostelium minutum*. Differentiation. 1985;28:205–8.
15. Galardi-Castilla M, Garciandia A, Suarez T, Sastre L. The *Dictyostelium discoideum acaA* gene is transcribed from alternative promoters during aggregation and multicellular development. PLoS ONE. 2010;5(10): e13286.
16. Verkerke-van Wijk I, Fukuzawa M, Devreotes PN, Schaap P. Adenylyl cyclase A expression is tip-specific in *Dictyostelium* slugs and directs StatA nuclear translocation and CudA gene expression. Dev Biol. 2001;234(1):151–60.
17. Faix J, Kreppel L, Shaulsky G, Schleicher M, Kimmel AR. A rapid and efficient method to generate multiple gene disruptions in *Dictyostelium discoideum* using a single selectable marker and the Cre-loxP system. Nucleic Acids Res. 2004;32(19): e143.
18. Paschke P, Knecht DA, Williams TD, Thomason PA, Insall RH, Chubb JR, Kay RR, Veltman DM. Genetic engineering of *Dictyostelium discoideum* cells based on selection and growth on bacteria. J Vis Exp Jove. 2019;143:58981.
19. Schulkes C, Schaap P. cAMP-dependent protein kinase activity is essential for preaggegative gene expression in *Dictyostelium*. FEBS Lett. 1995;368:381–4.
20. Kawabe Y, Schilde C, Du Q, Schaap P. A conserved signalling pathway for amoebozoan encystation that was co-opted for multicellular development. Sci Rep. 2015;5:9644.
21. Dinauer MC, Steck TL, Devreotes PN. Cyclic 3′,5′-AMP relay in *Dictyostelium discoideum* V adaptation of the cAMP signaling response during cAMP stimulation. J Cell Biol. 1980;86:554–61.
22. Tomchik KJ, Devreotes PN. Adenosine 3′,5′-monophosphate waves in *Dictyostelium discoideum*: a demonstration by isotope dilution-fluorography. Science. 1981;212:443–6.
23. Vaughan R, Pupillo M, Theibert A, Klein P, Devreotes P. Surface receptor mediated activation and adaptation of adenylate cyclase in *Dictyostelium discoideum*. In: Konijn TM, editor. Molecular mechanisms of desensitization to signal molecules NATO ASI series. 6th ed. Berlin: Springer-Verlag; 1987.
24. Sun TJ, Van Haastert PJM, Devreotes PN. Surface cAMP receptors mediate multiple responses during development in *Dictyostelium*: evidenced by antisense mutagenesis. JCell Biol. 1990;110:1549–54.
25. Sucgang R, Weijer CJ, Siegert F, Franke J, Kessin RH. Null mutations of the *Dictyostelium* cyclic nucleotide phosphodiesterase gene block chemotactic cell movement in developing aggregates. Dev Biol. 1997;192:181–92.
26. Alvarez-Curto E, Weening KE, Schaap P. Pharmacological profiling of the *Dictyostelium* adenylate cyclases ACA. ACB and ACG Biochem J. 2007;401(1):309–16.
27. Kesbeke F, Van Haastert PJM, Schaap P. Cyclic AMP relay and cyclic AMP-induced cyclic GMP accumulation during development of *Dictyostelium discoideum*. FEMS MicrobiolLett. 1986;34:85–9.
28. Gloeckner G, Lawal HM, Felder M, Singh R, Singer G, Weijer CJ, Schaap P. The multicellularity genes of dictyostelid social amoebas. Nat Commun. 2016;7:12085.
29. Pitt GS, Milona N, Borleis J, Lin KC, Reed RR, Devreotes PN. Structurally distinct and stage-specific adenylyl cyclase genes play different roles in *Dictyostelium* development. Cell. 1992;69:305–15.
30. Saran S, Schaap P. Adenylyl cyclase G is activated by an intramolecular osmosensor. Mol Biol Cell. 2004;15(3):1479–86.
31. Alvarez-Curto E, Saran S, Meima M, Zobel J, Scott C, Schaap P. cAMP production by adenylyl cyclase G induces prespore differentiation in *Dictyostelium* slugs. Development. 2007;134(5):959–66.
32. Van Es S, Virdy KJ, Pitt GS, Meima M, Sands TW, Devreotes PN, Cotter DA, Schaap P. Adenylyl cyclase G, an osmosensor controlling germination of *Dictyostelium* spores. J Biol Chem. 1996;271:23623–5.
33. Soderbom F, Anjard C, Iranfar N, Fuller D, Loomis WF. An adenylyl cyclase that functions during late development of *Dictyostelium*. Development. 1999;126:5463–71.
34. Kriebel PW, Parent CA. Adenylyl cyclase expression and regulation during the differentiation of *Dictyostelium discoideum*. IUBMB Life. 2004;56(9):541–6.
35. Comer FI, Parent CA. Phosphoinositide 3-kinase activity controls the chemoattractant-mediated activation and adaptation of adenylyl cyclase. Mol Biol Cell. 2006;17(1):357–66.
36. Maeda M, Lu S, Shaulsky G, Miyazaki Y, Kuwayama H, Tanaka Y, Kuspa A, Loomis WF. Periodic signaling controlled by an oscillatory circuit that includes protein kinases ERK2 and PKA. Science. 2004;304(5672):875–8.
37. Harwood AJ, Drury L. New vectors for expression of the *E.coli lacZ* gene in *Dictyostelium*. Nucl Acids Res. 1990;18:4292–4292.
38. Kawabe Y, Enomoto T, Morio T, Urushihara H, Tanaka Y. LbrA, a protein predicted to have a role in vesicle trafficking, is necessary for normal morphogenesis in *Polysphondylium pallidum*. Gene. 1999;239(1):75–9.
39. Dingermann T, Reindl N, Werner H, Hildebrandt M, Nellen W, Harwood A, Williams J, Nerke K. Optimization and in situ detection of *Escherichia coli* beta-galactosidase gene expression in *Dictyostelium discoideum*. Gene. 1989;85:353–62.
40. Gilman AG. Protein binding assays for cyclic nucleotides. Adv Cyc Nuc Res. 1972;2:9–24.

Publisher's Note